Author/s:
Zhang, Y-J;Hu, H-W;Yan, H;Wang, J-T;Lam, SK;Chen, Q-L;Chen, D;He, J-Z

Title:
Salinity as a predominant factor modulating the distribution patterns of antibiotic resistance genes in ocean and river beach soils

Date:
2019-06-10

Citation:
Zhang, Y. -J., Hu, H. -W., Yan, H., Wang, J. -T., Lam, S. K., Chen, Q. -L., Chen, D. & He, J. -Z. (2019). Salinity as a predominant factor modulating the distribution patterns of antibiotic resistance genes in ocean and river beach soils. Science of the Total Environment, 668, pp.193-203. https://doi.org/10.1016/j.scitotenv.2019.02.454.

Persistent Link:
https://hdl.handle.net/11343/291500

Elsevier Editorial System(tm) for Science of the Total Environment

Manuscript Draft

Manuscript Number: STOTEN-D-18-13980R1

Title: Salinity as a predominant factor modulating the distribution patterns of antibiotic resistance genes in ocean and river beach soils

Article Type: Research Paper

Keywords: soil resistome; soil salinity; beach soils; bacterial community; public health

Corresponding Author: Dr. Hangwei Hu,

Corresponding Author's Institution: The University of Melbourne

First Author: Yujing Zhang

Order of Authors: Yujing Zhang; Hangwei Hu; Hui Yan, PhD; Juntao Wang, PhD; Shu Kee Lam, PhD; Qinglin Chen, PhD; Deli Chen, PhD; Jizheng He, PhD

Abstract: Growing evidence points to the pivotal role of the environmental factors in influencing the transmission of antibiotic resistance genes (ARGs) and the propagation of resistant human pathogens. However, our understanding of the ecological and evolutionary environmental factors that contribute to development and dissemination of antibiotic resistance is lacking. Here, we profiled a wide variety of ARGs using the high-throughput quantitative PCR analysis in 61 soil samples collected from ocean and river beaches, which are hotspots for human activities and platforms for potential transmission of environmental ARGs to human pathogens. We identified the dominant abiotic and biotic factors influencing the diversity, abundance and composition of ARGs in these ecosystems. A total of 110 ARGs conferring resistance to eight major categories of antibiotics were detected. The core resistome was mainly affiliated into beta-lactam and multidrug resistance, accounting for 66.9% of the total abundance of ARGs. The oprJ gene conferring resistance to multidrug was the most widespread ARG subtype detected in all the samples. The relative abundances of total ARGs and core resistome were significantly correlated with salinity-related properties including electrical conductivity and concentrations of sodium and chloride. Random forest analysis and structural equation modeling revealed that salinity was the most important factor modulating the distribution patterns of beach soil ARGs after accounting for multiple drivers. These findings suggest that beach soil is a rich reservoir of ARGs and that salinity is a predominant factor shaping the distribution patterns of soil resistome.

Response to Reviewers: Please see attached responses to reviewer comments.

*Graphical Abstract

Graphical abstract

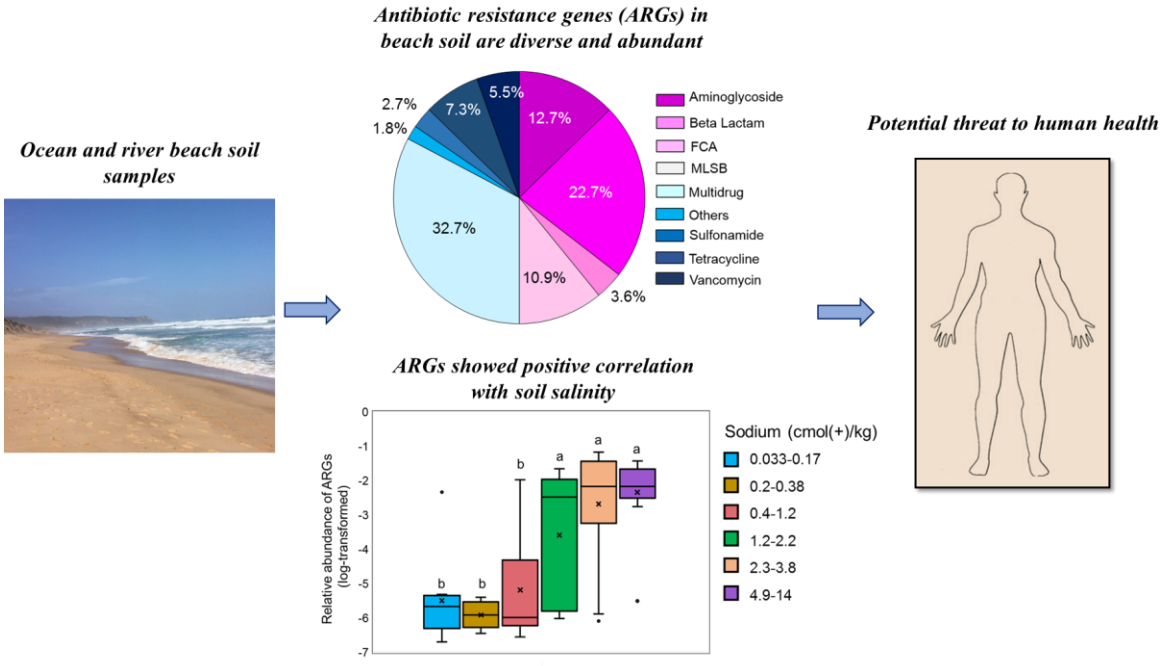

Highlights

- Ocean and river beach soils are important reservoirs of antibiotic resistance genes (ARGs)
- The *oprJ* gene is the most widespread ARG in beach soils
- Beach soils in different geographical locations shared extensive core resistome
- The abundance of ARGs had a significantly positive correlation with soil salinity properties
- Salinity is the most important factor modulating the distribution patterns of beach soil ARGs

Title page

Salinity as a predominant factor modulating the distribution patterns of antibiotic resistance genes in ocean and river beach soils

Yu-Jing Zhang[1], Hang-Wei Hu[1,*], Hui Yan[2], Jun-Tao Wang[3], Shu Kee Lam[1], Qing-Lin Chen[1], Deli Chen[1], Ji-Zheng He[1, 3]

[1] *Faculty of Veterinary and Agricultural Sciences, The University of Melbourne, Parkville, VIC 3010, Australia*

[2] *College of Animal Science and Technology, Hebei Agricultural University, Baoding 071000, China*

[3] *State Key Laboratory of Urban and Regional Ecology, Research Centre for Eco-Environmental Sciences, Chinese Academy of Sciences, Beijing 100085, China*

*Author for correspondence: Hang-Wei Hu, E-mail: hang-wei.hu@unimelb.edu.au

Running head: Salinity is an important environmental factor of soil resistome

Abstract

Growing evidence points to the pivotal role of the environmental factors in influencing the transmission of antibiotic resistance genes (ARGs) and the propagation of resistant human pathogens. However, our understanding of the ecological and evolutionary environmental factors that contribute to development and dissemination of antibiotic resistance is lacking. Here, we profiled a wide variety of ARGs using the high-throughput quantitative PCR analysis in 61 soil samples collected from ocean and river beaches, which are hotspots for human activities and platforms for potential transmission of environmental ARGs to human pathogens. We identified the dominant abiotic and biotic factors influencing the diversity, abundance and composition of ARGs in these ecosystems. A total of 110 ARGs conferring resistance to eight major categories of antibiotics were detected. The core resistome was mainly affiliated into β-lactam and multidrug resistance, accounting for 66.9% of the total abundance of ARGs. The *oprJ* gene conferring resistance to multidrug was the most widespread ARG subtype detected in all the samples. The relative abundances of total ARGs and core resistome were significantly correlated with salinity-related properties including electrical conductivity and concentrations of sodium and chloride. Random forest analysis and structural equation modeling revealed that salinity was the most important factor modulating the distribution patterns of beach soil ARGs after accounting for multiple drivers. These findings suggest that beach soil is a rich reservoir of ARGs and that salinity is a predominant factor shaping the distribution patterns of soil resistome.

Keywords: soil resistome; soil salinity; beach soils; bacterial community; public health

1. Introduction

The development of bacterial resistance to antimicrobials is a preeminent challenge to global public health and a major threat to modern medicine in the 21st century (Levy et al., 2004; Berendonk et al., 2015; Van Goethem et al., 2018). The antimicrobials used in human medicines and livestock production, and antimicrobial residues and heavy metals derived from land application of animal manures and municipal wastes are considered as the major selective pressures on the proliferation of environmental antibiotic resistance genes (ARGs) (Graham et al., 2010; Zhu et al., 2013). However, these selective pressures cannot fully explain the widespread occurrence of ARGs in natural environments with minimal anthropogenic disturbance (Allen et al., 2009; D'Costa et al., 2011; Forsberg et al., 2014; Hu et al., 2018). The emergence of environmental ARGs is a naturally occurring phenomenon that predates the era of antibiotic (Martínez, 2008; Cox and Wright, 2013), suggesting that some environmental factors, other than antibiotics, may contribute to the evolution, maintenance and proliferation of ARGs in natural environments. An improved understanding of the ecological factors that drive antibiotic resistance is necessary for predicting resistance dissemination and developing effective management strategies.

The roles of bacterial phylogeny and heavy metals have been well documented (Forsberg et al., 2014; Hu et al., 2016; Hu et al., 2017; Knapp et al., 2017), but we have limited understanding of the contribution of other environmental factors to the profiles of soil antibiotic resistance. There has been evidence that alterations in soil salt concentrations, nutrient status and pH imposed selection pressures on the evolution of bacterial communities, and were linked to the emergence of antibiotic resistance (Lauber et al., 2008; Poole, 2012; Rodriguez-Verdugo et al., 2013; Cruz-Loya et al., 2018). Cellular responses to temperature stress, nutrient starvation, oxidative and nitrosative stresses are often paralleled with concurrent responses to antibiotics, as these stresses and antimicrobials are targeting same cellular components and processes (Poole, 2012). Theoretically, it is inefficient for a

67 microorganism to evolve independent resistance to every single stress it encounters, which
68 requires investment in protein production, genetic materials and energy (Cruz-Loya et al.,
69 2018). The evolutionary strategy of bacteria to cope with multiple environmental stresses,
70 therefore, suggests that the mechanisms that bacteria confer resistance to environmental
71 stresses might be co-opted to respond to antimicrobials stress as well.

72 Ocean and river beach soil environments are hotspots for human activities, with around
73 50% of the global population living within 100 km of coastlines (Zhu et al., 2017), and thus
74 are an important interface between environmental and human resistomes. Despite the
75 potential risk of antibiotic resistance dissemination, the profiles of ARGs in beach soils
76 remain largely understudied. The beach soil environment is generally characterized by high
77 salinity, as indicated by the concentrations of Na^+, Ca^{2+}, Mg^{2+} and anions Cl^-, SO_4^{2-}, CO_3^{2-}
78 , NO_3^- and electrical conductivity (Shi et al., 2005). A number of studies have reported that
79 changes in soil salinity significantly influence the microbial community structure (Wichern et
80 al., 2006; Canfora et al., 2014), but empirical evidence of the effect of salinity on soil
81 resistome is lacking. Here, by employing high-throughput quantitative PCR (HT-qPCR) to
82 profile a large spectrum of ARGs in soil samples collected from 61 ocean and river beaches
83 in Victoria, Australia, we sought to quantify the soil resistome and identify the major abiotic
84 and biotic factors shaping its distribution patterns.

85 **2. Materials and methods**

86 ***2.1. Soil sampling and DNA extraction***

87 Soil samples were collected from 42 ocean beaches with a high volume of tourists
88 along 600 km of shoreline of Port Philip Bay and from 19 river beaches along 100 km of
89 Yarra River in Victoria, Australia, in August 2017 (Figure S1). All the sampling sites were
90 within the urban area and closely related to human activities. Detailed information for
91 sampling sites was provided in Table S1. At each site, one soil sample (0-15 cm, a composite

of five soil cores) was collected and transported to the laboratory on ice. Soil samples were passed through a 2.0 mm sieve for analysis of physicochemical properties and stored at -80 °C before molecular analysis. Soil DNA was extracted from 0.25 g soil using the MoBio PowerSoil DNA extraction kit (MoBio Laboratories, Carlsbad, CA, USA) following the manufacturer's instructions. The extracted DNA was checked for concentration (> 15ng μl^{-1}) and purity (A260/A280 ratio > 1.8 and A260/230 ratio > 2.0) by NanoDrop 2000c spectrophotometer (Thermo Scientific, Waltham, MA, UK).

2.2. Soil physicochemical characterization

Electrical conductivity (EC), sodium and chloride concentrations were used as indicators of soil salinity. EC was measured in soil suspension with a soil to water ratio of 1:5. Sodium concentration was determined by the ammonium acetate method (Schollenberger and Simon, 1945). Chloride concentration was measured using the single column ion chromatography (Hern et al., 1983). Soil total nitrogen and total carbon were measured using the Dumas combustion method using the isotope-ratio mass spectrometry (Sercon Hydra, Crewe, UK). Ammonium, nitrate (both extracted with 2 M KCl) and Colwell phosphorus (extracted with 0.5 M $NaHCO_3$) concentrations were determined by a Segmented Flow Analyzer (SAN++, Skalar, Breda, NL). Soil organic matter was determined by the Walkley-Black titration method. The diethylenetriaminepentaacetic acid (DTPA) extraction method was used to determine the concentrations of targeted heavy metals, including copper, zinc, iron, and manganese (Kulikov, 2016). Soil pH was determined in soil suspension with a soil to water ratio of 1:5 using a Delta 320 pH-meter (Mettler-Toledo Instruments, Columbus, OH, USA).

2.3. High-throughput quantitative PCR (HT-qPCR) analysis

The HT-qPCR analysis was conducted to quantify ARGs and mobile genetic elements (MGEs) using the thermal cycling conditions as described previously (Su et al., 2015; Zhang et al., 2017). The HT-qPCR array had 296 primer sets (Su et al., 2015; Hu et al., 2016), including 285 primer sets targeting eight major categories of ARGs, eight transposon-transposases, one class 1 integron-integrase, one clinical class 1 integron-integrase and one 16S rRNA gene. All DNA samples were diluted to 15 ng μl^{-1} using sterile water and analysed in triplicate for each sample on the Wafergen SmartChip Real-time PCR system (Fremont, CA, USA). Only well data with single effective melting peak and the amplification efficiencies within 1.7-2.3 for three replicates were regarded as positive and retained for further analysis. A threshold cycle (C_T) value of 31 was used as the detection limit (Su et al., 2015). The comparative C_T method, also referred to as the $2^{-\Delta C_T}$ method of relative profiling, was used to calculate the relative abundances of ARGs and MGEs compared to the 16S rRNA gene using the equations below (Schmittgen and Livak, 2008).

$$\Delta C_T = C_{T\,(ARG)} - C_{T\,(16S)} \quad (1)$$

$$\text{Relative abundance} = 2^{-\Delta C_T} \quad (2)$$

where C_T is the threshold cycle, ARG denotes one of the detected antibiotic-resistance gene assays, and 16S denotes the 16S rRNA gene assay.

2.4. Miseq sequencing and data processing

The V4 region of the 16S rRNA gene was targeted using the primer pair 515F (GTGCCAGCMGCCGCGGTAA) and 806R (GGACTACHVHHHTWTCTAAT) (Bates et al., 2011) with overhang adaptor sequences following the protocols as described in Gou et al. (2018). The 25 μl reaction mixture contained 12.5 μl of Redmix (Bioline, London, UK), 0.5 μl of each primer (10 μM), 9.5 μl of RNase-free water, and 2 μl of DNA (~15ng μl^{-1}). The thermal-cycling conditions were 95 °C for 10 min, and 25 cycles of 95 °C for 20 s, 55 °C for 20 s and 72 °C for 20 s. PCR products were purified using the Agencourt AMPure XP beads

(Beckman Coulter, Beverly, MA, USA). The final library by pooling all PCR products in equimolar ratios was sequenced using 2×300-bp paired-end strategy on the Illumina MiSeq platform in University of Melbourne.

Raw paired-end sequences were assembled after removing low-quality reads, adaptor sequences and ambiguous nucleotides using the Fast Length Adjustment of Short Reads (FLASH) (Magoè and Salzberg, 2011). Quantitative Insights Into Microbial Ecology (QIIME) analysis was performed to de-multiplex and assign merged sequences to individual samples (Caporaso et al., 2010). The operational taxonomic units (OTUs) were defined at a 97% similarity level using UCLUST (Edgar, 2010). Chimeric sequences and singleton OTUs were removed. Taxonomic classification of OTUs was performed against the 16S rRNA database of Greengenes version 13.5 (McDonald et al., 2012), and a set of representative sequences from each OTU were aligned using a PyNAST aligner (Langille et al., 2013). Sequences were randomly selected to the same number of reads (30,000 reads) per sample to compensate for the variation in sequencing depth prior to downstream analysis.

2.5 Extraction of the core resistome and microbiome

Here, the most abundant (top 50% most abundant ARG subtypes) and highly shared (present in > 50 % samples) ARGs were defined as core resistome, and the bacterial OTUs that were highly abundant (top 10% most abundant) and ubiquitous (presented in > 50% samples) were defined as core microbiome, respectively (Delgado-Baquerizo et al., 2018). The relative abundance of ARGs and normalized OTU tables were used to extract core resistome and core microbiome, respectively.

2.6. Statistical analyses and data visualization

The spatial distributions of ARGs in soil samples were plotted using the geographic information system ArcGIS 9.3. Heatmap showing the relative abundance of individual ARG subtypes was generated in R 3.2.5 (http://cran.r-project.org/) using the “pheatmap” package

(Kolde, 2012). The difference in the bacterial community compositions across sampling sites was visualized by non-metric multidimensional scaling (NMDS) ordinations based on the Bray-Curtis dissimilarity distances using the "vegan" package in R (Oksanen et al., 2017). Post-hoc plot was generated to compare the bacterial communities between ocean and river beach soils using the STAMP V2.1.3 (Parks et al., 2014). The correlations between ARG classes and MGEs were analysed using Mantel test using the "vegan" package with 999 permutations in R. Spearman's correlation test was conducted to analyze the relationships between the relative abundance of ARGs with MGEs and soil properties in SPSS 19.0. We visualized the correlations between ARGs and MGEs in a correlation matrix by calculating all possible pairwise Spearman's rank correlations between ARG subtypes (with a minimum occurrence of three across all the soil samples) and MGEs. A correlation was considered as statistically robust with a correlation coefficient > 0.8 and a significant level < 0.01 (Junker and Schreiber, 2008). The resultant correlation matrix was translated into an association network using the Fruchterman Reingold algorithm on the interaction platform of Gephi 0.9.1 (Bastian et al., 2009).

2.7. Random forest analysis and structural equation modelling (SEM)

We carried out Random forest analysis to identify the main predictors of ARG abundances among the following predictors: MGEs, soil salinity (EC, chloride and sodium), soil fertility (total nitrogen, total carbon, ammonium, nitrate, Colwell phosphorus and organic matter), heavy metals (copper, zinc, iron, and manganese) and microbial diversity (Shannon index). The importance of each predictor was determined by the increase in the mean square error (InMSE), which was computed for each tree and averaged across 5000 trees (Delgado-Baquerizo et al., 2016). The significance of the importance of each predictor on ARG profiles was estimated by using the *rfPermute* package (Archer, 2013) in R.

The structural equation model (SEM) was constructed to evaluate the effects of potential environmental factors including soil salinity, soil fertility, heavy metals, MGEs, and microbial diversity, as well as sample types (ocean or river beach soils) on the ARG patterns (Grace, 2006). An *a prior* model was established based on the known relationships among these drivers and ARG abundances (Fig. S2). The correlations among these variables were calculated with Mantel test using the "Ecodist" package in R (Goslee and Urban, 2007), and the resultant covariance matrix was parameterized into AMOS Graphics software (AMOS IBM, USA) for the SEM construction. The goodness-of-fit index (GIF > 0.90), χ^2 test (P > 0.05), comparative fit index (CIF = 0 ~ 1) and the root mean square errors of approximation (RMSEA < 0.05) were used to assess the overall goodness of the model fit. We calculated standardized total effects of each factor on the ARG patterns by summing all direct and indirect pathways between each factor and ARGs.

3. Results

3.1. Diversity and abundance of resistome in beach soil environments

A total of 110 ARGs and 8 MGEs were detected by the HT-qPCR array across all the samples (Table S2). The two most frequently detected ARG classes, conferring resistance to multidrug and β-lactam, accounted for 32.7% and 22.7% of the total numbers of detected ARGs, respectively (Fig. 1a). The other frequently detected ARG categories included aminoglycoside (12.7%), MLSB (10.9%) and tetracycline (7.3%) (Fig. 1a). The detected ARGs represented three major resistance mechanisms: efflux pump (42.7%), antibiotic deactivation (40.9%) and cellular protection (15.5%) (Fig. 1b).

The genes conferring resistance to multidrug and β-lactam shared the highest relative abundances among all the samples (Fig. 1c and 1d). The multidrug resistance genes were more predominant in the river beach soils (sites Y1-Y19) than in the ocean beach soils (sites

B1-B42), while the opposite pattern was observed for aminoglycoside resistance genes (Fig. 1d). The patterns of the relative abundances of individual ARG and MGE subtypes across all the beach soil samples were explored in a heatmap (Fig. 2). All the soil samples (columns in the heatmap) were generally separated into two major clusters with cluster I harboring 27 ocean beach soils and the cluster II including 34 soil samples collected from both ocean and river beaches (Fig. 2). The boxplot further showed that the soil samples in the Cluster I harbored significant higher relative abundance of ARGs compared with Cluster II ($P < 0.01$) (Fig. S3).

3.2. Characterization of the soil microbiome

Miseq sequencing of the 16S rRNA gene yielded a total of 1,765,450 high-quality sequences from all the samples, which clustered into 18,352 OTUs at 97% sequence identity. Proteobacteria, Actinobacteria, Planctomycetes and Bacteroidetes were the dominant phyla (Fig. 3a), accounting for 71.7 % of the total bacterial sequences (Fig. 3a). The most abundant 20 classes were mainly grouped into the phyla Proteobacteria, Actinobacteria, Acidobacteria and Bacteroidetes, with Gammaproteobacteria, Actinobacteria and Alphaproteobacteria being the three most abundant classes (Fig. 3c). The Actinobacteria phylum was significantly more abundant in the river beach soil samples than in the ocean beach soil samples ($P < 0.01$), while the opposite was observed for Planctomycetes and Bacteroidetes ($P < 0.01$) (Fig. 3b). The non-metric multidimensional scaling (NMDS) ordination analysis based on the Bray-Curtis distance metrics further suggests that the bacterial communities differed between the ocean and river beach soil samples (Fig. S4). The abundances of 24 bacterial classes including Gammaproteobacteria, Actinobacteria, and Alphaproteobacteria, were significantly different between the ocean and river beach soils (Fig. S5).

3.3. Identification of the core resistome and core microbiome

Among the 50% most abundant ARG subtypes (55 out of 110 detected ARGs), 38 ARGs were found in more than 50% of sampling sites (31 out of 61 sites), accounting for 66.9% of the relative abundance of total ARGs across all the samples (Fig. 4a). These abundant and prevalent ARG subtypes were defined as the core resistome in this study (Fig. 2). The genes dominating the core resistome were associated with β-lactam, multidrug, MLSB, vancomycin and aminoglycoside resistance (Fig. 4b). The resistance genes *aacC*, bla_{TEM} and *oprJ* were the most abundant gene subtypes across all the soil samples (Fig. S6).

About 2.2 % of the bacterial phylotypes (411 out of 18,352 phylotypes) were highly abundant (top 10%) and present in > 50% soil samples (Fig. S7a), accounting for 41.8% of the 16S rRNA gene sequences across all the soil samples (Fig. S7a). Similar to the whole microbiome profiles, these core components of the soil microbiome were separated by sample types (Fig. S8). The core microbiomes belonged to 24 dominant classes that were affiliated into 9 phyla, of which Proteobacteria, Cyanobacteria, Bacteroidetes and Actinobacteria were the most abundant ones (Fig. S7b). At the class level, the most prevalent groups were Gammaproteobacteria, Chloroplast, Flavobacteria, Actinobacteria and Planctomycetia (Fig. S7b).

3.4. Correlations between ARGs and MGEs

The relative abundances of MGEs were consistently high across all the soil samples (Fig. 1c and 1d). In the network analysis, intensive correlations were observed among different ARG subtypes and MGEs (Fig. 5a). A modularity index of 0.565 suggested an obvious modular structure (Newman, 2006) with nine modules (Fig. 5b). ARGs in each module connected intensively with each other, especially in the three largest modules (modules I, II, III). The *aacC*, *cphA1* and bla_{ROB} genes were the most densely connected nodes in the three modules, which were defined as the “hubs” and used as the indicators of

the co-occurring ARGs in the same module (Li et al., 2015) (Table S3). Moreover, *aacC* and *cphA1* and many co-occurred ARGs were also the members of core resistome (Table S3). The *intI1*, *tnpA1*, *tnpA2* and *tnpA3* genes belonging to MGEs were clustered into different modules and intensively associated with ARGs (Fig. 5b). Mantel test further revealed that the relative abundances of MGEs were significantly and positively correlated with total ARGs, core resistome and individual ARG types (except multidrug) (Table S4).

3.5. Relationships between soil properties with ARGs, core resistome and MGEs

The relationships between resistome and soil properties including soil pH, soil salinity (sodium, chloride and EC), soil fertility (total carbon, total nitrogen, nitrate nitrogen, ammonium nitrogen, phosphorus, and organic matter) and heavy metals (copper, iron, manganese and zinc) were examined via Spearman's correlation analysis (Table 1). The relative abundances of total ARGs, core resistome and MGEs were all significantly and positively correlated with soil salinity-related variables ($P < 0.01$) (Table 1). On the contrary, most of the soil fertility indicators and heavy metals showed significant and negative correlations with the relative abundance of ARGs, core resistome and MGEs ($P < 0.05$). No significant correlations were found between soil pH and total ARGs or core resistome (Table 1). The changes in the relative abundances of ARGs and MGEs along the gradient of soil salinity were further explored in the boxplots (Fig. 6). All the 61 soil samples were affiliated into six salinity gradients according to their salt contents. The relative abundance of ARGs and MGEs significantly increased with the concentrations of sodium (Fig. 6a and 6d), chloride (Fig. 6b and 6e) and EC (Fig. 6c and 6f). Similarly, the relative abundance of core resistome significantly increased with soil salinity ($P < 0.05$) (Fig. S9).

3.6. The effect of soil salinity on ARG patterns when accounting for multiple factors

Random forest modelling indicated that MGEs and all the soil salinity-related variables were significant indicators of the ARG profiles ($P < 0.05$) (Fig. S10a) whereas only MGEs significantly influenced the abundance of core resistome ($P < 0.05$) (Fig. S10b). Soil salinity and MGEs were important predictors of the ARG profiles after accounting for the direct and indirect effects of multiple variables (Fig. 7). Our SEM explained 95% of the variance in the ARG abundance across the ocean and river beach soils (Fig. 7a). Soil salinity-related variables including EC and chloride concentration showed the highest positive effects on the ARG abundance (Fig. 7b). No significant direct effects of soil fertility or heavy metals were found on the ARG patterns. Sample types had indirect effects on ARGs through its significant impacts on soil salinity, MGEs, and the microbial diversity (Fig. 7a). EC could also affect the ARG patterns indirectly via its positive effects on MGEs (Fig. 7a). The SEM of core resistome showed similar results with those of total ARGs (Fig. S11).

4. Discussion

4.1 Beach soil resistome is diverse and susceptible to horizontal gene transfer

The ARGs observed in our study were abundant and diverse, indicating that beach soils are important reservoirs of antibiotic resistance. In line with previous studies of ARGs in China estuaries (Zhu et al., 2017), urban sewage (Su et al., 2015), forest soils (Hu et al., 2018), and urban soils (Xiang et al., 2018), genes conferring resistance to β-lactam and multidrug are the most dominant ARG subtypes in these beach soils. Identification of the core resistome (67% of the total abundance of ARGs detected across all the samples, Fig. 4) indicated that beach soils in different geographical locations shared extensive antibiotic resistome. Several ARG subtypes affiliated to the core resistome, such as bla_{TEM}, *fox5*, $bla_{CTX\text{-}M\text{-}04}$, bla_{SFO}, *oprJ*, *oprD*, *acrA5*, *mphA1*, *vanC3* and *aacC* genes, were ubiquitously detected in high abundance across most of the soil samples (Fig. 4b and S5). The bla_{TEM} gene (β-lactam resistance) was the most abundant ARG in our study and has been detected in remote

soil environments in the absence of anthropogenic activities and use of antibiotics (Allen et al., 2009). The *oprJ*, *oprD* and *acrA5* genes conferring resistance to multidrug may be potentially driven by multiple intrinsic antibiotics in soils. The *aacC* gene was found to be widely distributed in various genera including *Aeromonas*, *Escherichia*, *Vibrio*, *Salmonella*, and *Listeria spp*. isolated from polluted or natural water environments (Zhang et al., 2009). The *vanC3* gene confers resistance to vancomycin, which is regarded as the last weapon to defend *Staphylococcus aureus* (Gilmore and Hoch, 1999; Hu et al., 2018). Unfortunately, the vancomycin-resistant *S. aureus* strains have been detected from most parts of the world (Walsh and Howe, 2002). All these findings suggest that beach soils harbored an extensive core resistome including clinical-related ARGs and may pose a health risk to humans via direct contact. The identification of core resistome can provide a more reliable prediction of the dissemination of antibiotic resistance in environmental settings.

The MGEs were detected in consistently high abundance and were significantly correlated with total ARGs, core resistome and different classes of ARGs. This suggests a potential for horizontal transfer of ARGs in beach soils. The class 1 integrase gene *intI1* and the transposase genes *tnpA1*, *tnpA2* and *tnpA3* were intensively associated with multiple ARGs encoding resistance to different categories of antibiotics including β-lactam, MLSB, tetracycline, multidrug and vancomycin (Fig. 2b). These co-occurring ARGs may be genetically associated with integrons, transposons or plasmids, likely enabling the movement of ARGs between different bacterial cells (Hu et al., 2018; Partridge et al., 2009). The HGT mediated by MGEs could uncouple the relationships between ARGs and the bacterial phylogeny (Forsberg et al., 2014), as suggested by the minor role of bacterial community in shaping the ARG profiles (Fig. S10). Our SEM found that MGEs were an important factor shaping the abundance of core resistome and total ARGs when simultaneously accounting for multiple soil properties and bacterial communities. These findings suggest that ARGs,

335 especially the core resistome, in beach soils are likely to be horizontally transferred, enabling
336 possible acquisition of antibiotic resistance in environmental bacteria and pathogens and the
337 dissemination of ARGs (Johnson et al., 2016).

338 ***4.2 Salinity as the most important environmental factor shaping the ARG patterns in beach***
339 ***soils***

340 In this study, soil salinity-related variables were identified as the significant predictors
341 of the ARG profiles ($P < 0.05$) (Fig. S10a). Although the effect of salinity-related properties
342 on core resistome was not significant (Fig. S10b), these factors were more important than all
343 the other environmental factors in predicting the core resistome patterns (Fig. S10b). Soil
344 salinity attributes were further identified as the most important environmental factors in
345 modulating the ARG distribution patterns in beach soil environments (Fig. 7). Much of our
346 understanding of the correlation between salinity and ARGs was derived from aquatic
347 ecosystems (Bergeron et al., 2016; Belding and Boopathy, 2018; Liu et al., 2018), with
348 limited reports of ARG responses to salinity stress in soils. We found a significant increasing
349 tendency of ARGs along the soil salinity gradients (Fig. 6), suggesting that bacteria might
350 have developed increased resistance to antibiotics during the evolution to cope with elevated
351 salinity stress. This finding was further supported by the SEM analysis, with the salinity
352 attribute EC showing a significant direct effect on ARGs (Fig. 7). Environmental stresses like
353 extreme temperature, pH and salinity can induce bacteria to cope with these stresses through
354 making phenotypic and genotypic adaptations, enabling resistance to similar stresses
355 subsequently (Storz and Hengge-Aronis, 2000). Therefore, we suggested that soil salinity as
356 an environmental stress may directly contribute to the evolution and prevalence of ARGs in
357 beach soil environments. Previous studies showed that bacteria tolerant to salinity stress often
358 had increased resistance to antibiotics (Gramegna et al., 2017; McMahon et al., 2006). A

359 microcosm incubation study indicated that high salinity increased antibiotic resistance in
360 food-related pathogens, even after removal of stress (McMahon et al., 2007). Salinity stress
361 may directly induce bacterial cells to develop resistance to antibiotics by means of increased
362 translation of multiple antibiotic resistance operons, transfer of ARGs-containing plasmid,
363 and increased expression of ARG-related bacterial proteins (Bishop, 2000; McMahon et al.,
364 2007).

365 Apart from the direct effect of salinity on ARGs, salinity attribute (EC) also indirectly
366 affects soil resistome through its positive effects on MGEs (Fig. 7). Moreover, soil salinity
367 may potentially impose indirect pressure on resistome by altering the solubility of soil
368 organic matter (Rath et al., 2018), mobility of heavy metals (Acosta et al., 2011), and soil pH
369 (Wong et al., 2010), which have been identified as important environmental abiotic factors of
370 resistome (Chen et al., 2018; Hu et al., 2016; Hu et al., 2017; McMahon et al., 2007;). More
371 importantly, salinity has been identified as a dominant factor structuring the community
372 compositions of soil microbes (Rath and Rousk, 2015). The filtering effect of salinity may
373 eliminate the salt-susceptible bacteria and only allow salt-tolerant bacteria to survive and
374 proliferate (Rath et al., 2018). The shifts in bacterial communities in response to soil salinity
375 may indirectly influence resistome as many bacteria are antibiotic producers or potential
376 hosts of ARGs (Davies and Davies, 2010).

377 This is the first study of a wide variety of ARGs in ocean and river beach soil
378 environments, providing insights into how the soil salinity influences the distribution and
379 dissemination of soil resistome. High salinity is regarded as one of the most devastating
380 environmental stresses to soil fertility (Rath et al., 2018), with negative consequences on
381 plant growth and soil microbial activity (Rath et al., 2015). Furthermore, the salinized areas
382 are increasing at a rate of 10% annually and it has been estimated that more than 50% of the
383 cultivated land will be salinized by the year 2050 (Jamil et al., 2011). Except the natural

processes (such as low precipitation, high surface evaporation, weathering of native rocks), irrigation with saline water and poor cultural practice were identified as two major human causes of arable land salinization (Shrivastava and Kumar, 2015). Our study suggests that saline soils might be an important platform for the evolution and development of antibiotic resistance. Therefore, more sustainable irrigation practice and farm management should be designed to cope with salinity stress to control the dissemination of ARGs in agricultural soil system. These findings challenge our previous perceptions that antibiotic use and organic waste application are the dominant causes of antibiotic resistance in terrestrial ecosystems (Chang et al., 2015; Zhang et al., 2017). The resistomes in natural ecosystems characterized by environmental stresses, such as beach soils with high salinity and soils contaminated by heavy metals, might have evolved and developed under the selection pressure of the dominant stresses.

5. Conclusions

This first attempt of exploring ARGs in ocean and river beach soil environments provides important evidence that soil salinity is critical to shaping the profiles of resistome in these ecosystems. Environmental stress such as salinity may enhance bacterial resistance to broad-spectrum antibiotics. Our findings have implications for public health considering the potential transmission of environmental ARGs to human pathogens or commensals under salinity-stressed conditions. Understanding the environmental stresses that maintain the environmental resistome is essential to the development of effective strategies to minimize the dissemination of ARGs.

Acknowledgements

This work was supported by Australian Research Council Discovery projects (DE150100870, DP170103628) and the Australia-China Joint Research Centre (ACSRF48165)

References

Acosta, J.A., Jansen, B., Kalbitz, K., Faz, A., Martínez-Martínez, S., 2011. Salinity increases mobility of heavy metals in soils. Chemosphere 85,1318-1324. https://doi.org/10.1016/j.chemosphere.2011.07.046.

Allen, H.K., Moe, L.A., Rodbumrer, J., Gaarder, A., Handelsman, J., 2009. Functional metagenomics reveals diverse β-lactamases in a remote Alaskan soil. The ISME Journal 3, 243. https://doi.org/10.1038/ismej.2008.86.

Archer, E., 2013. rfPermute: Estimate permutation p-values for Random Forest importance metrics. R package version 1.5. 2.

Bastian, M., Heymann, S., Jacomy, M., 2009. Gephi: an open source software for exploring and manipulating networks. Icwsm. 8, 361-362.

Bates, S.T., Berg-Lyons, D., Caporaso, J.G., Walters, W.A., Knight, R., Fierer, N., 2011. Examining the global distribution of dominant archaeal populations in soil. The ISME Journal 5, 908–917. https://doi.org/10.1038/ismej.2010.171.

Belding, C., Boopathy, R., 2018. Presence of antibiotic-resistant bacteria and antibiotic resistance genes in coastal recreational waters of southeast Louisiana, USA. Journal of Water Supply: Research and Technology-Aqua. https://doi.org/10.2166/aqua.2018.076.

Berendonk, T.U., Manaia, C.M., Merlin, C., Fatta-Kassinos, D., Cytryn, E., Walsh, F., Bürgmann, H., Sørum, H., Norström, M., Pons, M.N., 2015. Tackling antibiotic resistance: the environmental framework. Nature Reviews Microbiology 13, 310.

Bergeron, S., Brown, R., Homer, J., Rehage, S., Boopathy, R., 2016. Presence of antibiotic resistance genes in different salinity gradients of freshwater to saltwater marshes in southeast Louisiana, USA. International Biodeterioration & Biodegradation 113, 80-87. https://doi.org/10.1016/j.ibiod.2016.02.008.

Bishop, R.E., 2000. The bacterial lipocalins. Biochimica et Biophysica Acta (BBA)-Protein Structure and Molecular Enzymology 1482, 73-83. https://doi.org/10.1016/s0167-4838(00)00138-2.

Breiman, L., 2001. Random forest. Machine Learning 45, 5.

Canfora, L., Bacci, G., Pinzari, F., Papa, G.L., Dazzi, C., Benedetti, A., 2014. Salinity and bacterial diversity: to what extent does the concentration of salt affect the bacterial community in a saline soil? PLoS One 9: e106662. https://doi.org/10.1371/journal.pone.0106662.

Caporaso, J.G., Kuczynski, J., Stombaugh, J., Bittinger, K., Bushman, F.D., Costello, E.K., Fierer, N., Pena, A.G., Goodrich, J.K., Gordon, J.I., 2010. QIIME allows analysis of high-throughput community sequencing data. Nature Methods 7, 335.

Chang, Q., Wang, W., Regev-Yochay, G., Lipsitch, M., Hanage, W.P., 2015. Antibiotics in agriculture and the risk to human health: how worried should we be? Evolutionary applications 8, 240-247. https://doi-org.ezp.lib.unimelb.edu.au/10.1111/eva.12185.

Chen, Q.L., Fan, X.T., Zhu, D., An, X.L., Su, J.Q., Cui, L., 2018. Effect of biochar amendment on the alleviation of antibiotic resistance in soil and phyllosphere of Brassica chinensis L. Soil Biology and Biochemistry 119, 1-210. https://doi.org/10.1016/j.soilbio.2018.01.015.

Cox, G., Wright, G.D., 2013. Intrinsic antibiotic resistance: mechanisms, origins, challenges and solutions. International Journal of Medical Microbiology 303, 287-292. https://doi.org/10.1016/j.ijmm.2013.02.009.

Cruz-Loya, M., Kang, T.M., Lozano, N.A., Watanabe, R., Tekin, E., Damoiseaux, R., Savage, V.M., Yeh, P.J., 2018. Stressor interaction networks suggest antibiotic resistance co-opted from stress responses to temperature. The ISME journal p. 1. https://doi.org/10.1038/s41396-018-0241-7.

459 Davies, J., Davies, D., 2010. Origins and evolution of antibiotic resistance. Microbiology and
460 molecular biology reviews 74, 417-433. doi: 10.1128/MMBR.00016-10.
461 D'Costa, V.M., King, C.E., Kalan, L., Morar, M., Sung, W.W., Schwarz, C., Froese, D.,
462 Zazula, G., Calmels, F., Debruyne, R., Golding, G.B., 2011. Antibiotic resistance is
463 ancient. Nature 477, 457-461. https://doi.org/10.1038/nature10388.
464 Delgado-Baquerizo, M., Maestre, F.T., Reich, P.B., Jeffries, T.C., Gaitan, J.J., Encinar, D.,
465 Berdugo, M., Campbell, C.D., Singh, B.K., 2016. Microbial diversity drives
466 multifunctionality in terrestrial ecosystems. Nature Communications 7, 10541.
467 https://doi.org/10.1038/ncomms10541.
468 Delgado-Baquerizo, M., Oliverio, A.M., Brewer, T.E., Benavent-González, A., Eldridge, D.J.,
469 Bardgett, R.D., Maestre, F.T., Singh, B.K., Fierer, N., 2018. A global atlas of the
470 dominant bacteria found in soil. Science 359, 320-325.
471 https://doi.org/10.1126/science.aap9516.
472 Edgar, R.C., 2010. Search and clustering orders of magnitude faster than BLAST.
473 Bioinformatics 26, 2460-2461. https://doi.org/10.1093/bioinformatics/btq461.
474 Forsberg, K.J., Patel, S., Gibson, M.K., Lauber, C.L., Knight, R., Fierer, N., Dantas, G., 2014.
475 Bacterial phylogeny structures soil resistomes across habitats. Nature 509, 612.
476 https://doi.org/10.1038/nature13377.
477 Gilmore, M.S., Hoch, J.A., 1999. Antibiotic resistance: a vancomycin surprise. Nature 399,
478 524-526. https://doi.org/10.1038/21070.
479 Goslee, S.C., Urban, D.L., 2007. The ecodist package for dissimilarity-based analysis of
480 ecological data. Journal of Statistical Software 22, 1-19.
481 https://doi.org/10.18637/jss.v022.i07.
482 Gou, M., Hu, H.W., Zhang, Y.J., Wang, J.T., Hayden, H., Tang, Y.Q., He, J.Z., 2018. Aerobic
483 composting reduces antibiotic resistance genes in cattle manure and the resistome

dissemination in agricultural soils. The Science of Total Environment 612, 1300-1310. https://doi.org/10.1016/j.scitotenv.2017.09.028.

Grace, J.B., 2006. Structural Equation Modeling Natural Systems. Cambridge University Press.

Graham, D.W., Olivares-Rieumont, S., Knapp, C.W., Lima, L., Werner, D., Bowen, E., 2010. Antibiotic resistance gene abundances associated with waste discharges to the Almendares River near Havana, Cuba. Environmental Science & Technology 45, 418-424. https://doi.org/10.1021/es102473z.

Gramegna, A., Millar, B.C., Contarini, M., Blasi, F., Elborn, J.S., Downey, D.G., Moore, J.E., 2017. 193 In vitro synergistic effect of NaCl and antibiotics against P. aeruginosa from cystic fibrosis patients. Journal of Cystic Fibrosis 16, p.S116. https://doi.org/10.1016/s1569-1993(17)30557-x.

Hern, J., Rutherford, G., Vanloon, G., 1983. Determination of chloride, nitrate, sulphate and total sulphur in environmental samples by single-column ion chromatography. Talanta 30, 677-682. https://doi.org/10.1016/0039-9140(83)80155-6.

Hu, H.W., Wang, J.T., Li, J., Shi, X.Z., Ma, Y.B., Chen, D., He, J.Z., 2017. Long-term nickel contamination increases the occurrence of antibiotic resistance genes in agricultural soils. Environmental Science and Technology 51, 790-800. https://doi.org/10.1021/acs.est.6b03383.

Hu, H.W., Wang, J.T., Li, J., Li, J.J., Ma, Y.B., Chen, D., He, J.Z., 2016. Field-based evidence for copper contamination induced changes of antibiotic resistance in agricultural soils. Environmental Microbiology 18, 3896-3909. https://doi.org/10.1111/1462-2920.13370.

Hu, H.W., Wang, J.T., Singh, B.K., Liu, Y.R., Chen, Y.L., Zhang, Y.J., He, J.Z., 2018. Diversity of herbaceous plants and bacterial communities regulates soil resistome

across forest biomes. Environmental Microbiology 20, 3186-3220. https://doi.org/10.1111/1462-2920.14248.

Jamil, A., Riaz, S., Ashraf, M., Foolad, M.R., 2011. Gene expression profiling of plants under salt stress. Critical Reviews in Plant Sciences 30, 435-458. https://doi.org/10.1080/07352689.2011.605739.

Johnson, T.A., Stedtfeld, R.D., Wang, Q., Cole, J.R., Hashsham, S.A., Looft, T., Zhu, Y.G., Tiedje, J.M., 2016. Clusters of antibiotic resistance genes enriched together stay together in swine agriculture. MBio. 7, e02214-15. https://doi.org/10.1128/mbio.02214-15.

Knapp, C.W., Callan, A.C., Aitken, B., Shearn, R., Koenders, A., Hinwood, A., 2017. Relationship between antibiotic resistance genes and metals in residential soil samples from Western Australia. Environmental Science and Pollution Research 24, 2484-2494. https://doi.org/10.1007/s11356-016-7997-y.

Kolde, R., 2012. Pheatmap: pretty heatmaps. R package version 61.

Kulikov, E., 2016. Determination of elemental nutrients in DTPA extracted soil using the Agilent 5110 SVDV ICP-OES. Agilent publication.

Langille, M.G., Zaneveld, J., Caporaso, J.G., McDonald, D., Knights, D., Reyes, J.A., Clemente, J.C., Burkepile, D.E., Thurber, R.L.V., Knight, R., 2013. Predictive functional profiling of microbial communities using 16S rRNA marker gene sequences. Nature Biotechnology 31, 814. https://doi.org/10.1038/nbt.2676.

Lauber, C.L., Strickland, M.S., Bradford, M.A., Fierer, N., 2008. The influence of soil properties on the structure of bacterial and fungal communities across land-use types. Soil Biology and Biochemistry 40, 2407-2415. https://doi.org/10.1016/j.soilbio.2008.05.021.

533 Levy, S.B., Marshall, B., 2004. Antibacterial resistance worldwide: causes, challenges and
534 responses. Nature medicine 10, S122. https://doi.org/10.1038/nm1145.
535 Li, B., Yang, Y., Ma, L., Ju, F., Guo, F., Tiedje, J.M., Zhang, T., 2015. Metagenomic and
536 network analysis reveal wide distribution and co-occurrence of environmental
537 antibiotic resistance genes. The ISME Journal 9, 2490.
538 https://doi.org/10.1038/ismej.2015.59.
539 Liu, M., Li, Q., Sun, H., Jia, S., He, X., Li, M., Zhang, X.X., Ye, L., 2018. Impact of salinity
540 on antibiotic resistance genes in wastewater treatment bioreactors. Chemical
541 Engineering Journal 338, 557-563. https://doi.org/10.1016/j.cej.2018.01.066.
542 Magoè, T., Salzberg, S.L., 2011. FLASH: fast length adjustment of short reads to improve
543 genome assemblies. Bioinformatics 27, 2957–2963.
544 https://doi.org/10.1093/bioinformatics/btr507.
545 Martínez, J.L., 2008. Antibiotics and antibiotic resistance genes in natural environments.
546 Science 321, 365-367. https://doi.org/10.1126/science.1159483.
547 McDonald, D., Price, M.N., Goodrich, J., Nawrocki, E.P., DeSantis, T.Z., Probst, A.,
548 Andersen, G.L., Knight, R., Hugenholtz, P., 2012. An improved Greengenes taxonomy
549 with explicit ranks for ecological and evolutionary analyses of bacteria and archaea.
550 The ISME Journal 6, 610-8. https://doi.org/10.1038/ismej.2011.139.
551 McMahon, M.A.S,, Xu. J., Moore, J.E., Blair, I.S., McDowell, D.A., 2007. Environmental
552 stress and antibiotic resistance in food-related pathogens. Applied and Environmental
553 Microbiology 73, 211-217. https://doi.org/10.1128/aem.00578-06.
554 Newman, M.E., 2006. Modularity and community structure in networks. Proceedings of the
555 National Academy of Sciences 103, 8577-82.
556 https://doi.org/10.1073/pnas.0601602103

Oksanen, J., Guillaume Blanchet, F., Kindt, R., Legendre, P., 2017. Vegan: Community ecology package. R package version 2.3–5.

Parks, D.H., Tyson, G.W., Hugenholtz, P., Beiko, R.G., 2014. STAMP: statistical analysis of taxonomic and functional profiles. Bioinformatics 30, 3123-3124. https://doi.org/10.1658/1100-9233(2003)014[0927:vaporf]2.0.co;2.

Partridge, S.R., Tsafnat, G., Coiera, E., Iredell, J.R., 2009. Gene cassettes and cassette arrays in mobile resistance integrons. FEMS Microbiology Reviews 33, 757-784. https://doi.org/10.1111/j.1574-6976.2009.00175.x.

Poole, K., 2012. Stress responses as determinants of antimicrobial resistance in Gram-negative bacteria. Trends in Microbiology 20, 227-234. https://doi.org/10.1016/j.tim.2012.02.004.

Rath, K.M., Fierer, N., Murphy, D.V., Rousk, J., 2018. Linking bacterial community composition to soil salinity along environmental gradients. The ISME Journal 1. https://doi.org/10.1038/s41396-018-0313-8.

Rath, K.M., Rousk, J., 2015. Salt effects on the soil microbial decomposer community and their role in organic carbon cycling: a review. Soil Biology and Biochemistry, 81, 108-123. https://doi.org/10.1016/j.soilbio.2014.11.001.

Rodriguez-Verdugo, A., Faut, B.S., Tenaillon, O., 2013. Evolution of Escherichia coli rifampicin resistance in an antibiotic-free environment during thermal stress. BMC Evolutionary Biology 13, 50. https://doi.org/10.1186/1471-2148-13-50.

Schmittgen, T.D., Livak, K.J., 2008. Analyzing real-time PCR data by the comparative C_T method. Nature Protocols 3, 1101-1108. https://doi.org/10.1038/nprot.2008.73.

Schollenberger, C., Simon, R., 1945. Determination of exchange capacity and exchangeable bases in soil-ammonium acetate method. Soil Science 59, 13-24. https://doi.org/10.1097/00010694-194501000-00004.

582 Shi, D.C., Wang, D.L., 2005. Effects of various salt-alkaline mixed stresses on
583 Aneurolepidium chinense (Trin.) Kitag. Plant and Soil 271, 15-26.
584 https://doi.org/10.1007/s11104-004-1307-z.
585 Shrivastava, P., Kumar, R., 2015. Soil salinity: a serious environmental issue and plant
586 growth promoting bacteria as one of the tools for its alleviation. Saudi journal of
587 biological sciences 22, 123-131. https://doi.org/10.1016/j.sjbs.2014.12.001.
588 Storz, G., Hengge-Aronis, R., 2000. Bacterial stress responses. ASM Press, Washington, DC.
589 Su, J.Q., Wei, B., Ou-Yang, W.Y., Huang, F.Y., Zhao, Y., Xu, H.J., Zhu, Y.G., 2015. Antibiotic
590 resistome and its association with bacterial communities during sewage sludge
591 composting. Environmental Science and Technology 49, 7356-7363.
592 https://doi.org/10.1021/acs.est.5b01012.
593 Van Goethem, M.W., Pierneef, R., Bezuidt, O.K., Van De Peer, Y., Cowan, D.A.,
594 Makhalanyane, T.P., 2018. A reservoir of 'historical'antibiotic resistance genes in
595 remote pristine Antarctic soils. Microbiome 6, 40. https://doi.org/10.1186/s40168-
596 018-0424-5.
597 Wichern, J., Wichern, F., Joergensen, R.G., 2006. Impact of salinity on soil microbial
598 communities and the decomposition of maize in acidic soils. Geoderma 137, 100-108.
599 https://doi.org/10.1016/j.geoderma.2006.08.001.
600 Xiang, Q., Chen, Q.L., Zhu, D., An, X.L., Yang, X.R., Su, J.Q., Qiao, M., Zhu, Y.G., 2018.
601 Spatial and temporal distribution of antibiotic resistomes in a peri-urban area is
602 associated significantly with anthropogenic activities. Environmental Pollution 235,
603 525-533. https://doi.org/10.1016/j.envpol.2017.12.119.
604 Yan, N., Marschner, P., Cao, W., Zuo, C., Qin, W., 2015. Influence of salinity and water
605 content on soil microorganisms. International Soil and Water Conservation
606 Research 3, 316-323. https://doi.org/10.1016/j.iswcr.2015.11.003.

607 Zhang, Y.J., Hu, H.W., Gou, M., Wang, J.T., Chen, D., He, J.Z., 2017. Temporal succession of
608 soil antibiotic resistance genes following application of swine, cattle and poultry
609 manures spiked with or without antibiotics. Environmental Pollution 231, 1621-1632.
610 https://doi.org/10.1016/j.envpol.2017.09.074.
611 Zhang, X.X., Zhang, T., Fang, H.H., 2009. Antibiotic resistance genes in water
612 environment. Applied Microbiology and Biotechnology 82, 397-414.
613 https://doi.org/10.1007/s00253-008-1829-z.
614 Zhu, Y.G., Johnson, T.A., Su, J.Q., Qiao, M., Guo, G.X., Stedtfeld, R.D., Hashsham, S.A.,
615 Tiedje, J.M., 2013. Diverse and abundant antibiotic resistance genes in Chinese swine
616 farms. Proceedings of the National Academy of Sciences p.201222743.
617 https://doi.org/10.1073/pnas.1222743110.
618 Zhu, Y.G., Zhao, Y., Li, B., Huang, C.L., Zhang, S.Y., Yu, S., Chen, Y.S., Zhang, T., Gillings,
619 M.R., Su, J.Q., 2017. Continental-scale pollution of estuaries with antibiotic
620 resistance genes. Nature Microbiology 2, 16270.
621 https://doi.org/10.1038/nmicrobiol.2016.270.
622

Table 1 Spearman's correlations between the relative abundance of ARGs, core resistome and MGEs with soil properties.

		Soil salinity			**Heavy metals**			
		EC	Cl	Na	Cu	Fe	Zn	Mn
Total ARGs	ρ	**0.659****	**0.619****	**0.635****	-0.249	**-.268***	**-.317***	**-.373****
	Sig.	P < 0.01	P < 0.01	P < 0.01	P = 0.053	P = 0.037	P = 0.013	P < 0.01
Core resistome	ρ	**0.673****	**0.640****	**0.669****	**-0.411****	**-0.415****	**-0.467****	**-0.505****
	Sig.	P < 0.01	P < 0.01	P < 0.01	P < 0.01	P < 0.01	P < 0.01	P < 0.01
MGEs	ρ	**0.569****	**0.560****	**0.593****	**-0.414****	**-0.454****	**-0.473****	**-0.568****
	Sig.	P < 0.01	P < 0.01	P < 0.01	P < 0.01	P < 0.01	P < 0.01	P < 0.01

		Soil fertility						**Soil pH**
		TC	TN	NN	AN	OM	P	
Total ARGs	ρ	**-0.304***	**-0.321***	**-0.296***	-0.12	**-0.342****	**-0.317***	0.034
	Sig.	P = **0.017**	P = **0.012**	P = **0.021**	P = 0.358	P < 0.01	P = 0.013	P=0.793
Core resistome	ρ	**-0.323***	**-0.477****	**-0.429****	**-0.284***	**-0.503****	**-0.416****	0.250
	Sig.	P = 0.011	P < 0.01	P < 0.01	P = 0.027	P < 0.01	P < 0.01	P=0.052
MGEs	ρ	**-0.432****	**-0.546****	**-0.502****	**-0.354****	**-0.538****	**-0.498****	**0.287***
	Sig.	P < 0.01	P < 0.01	P < 0.01	P < 0.01	P < 0.01	P < 0.01	P=0.025

Bold text indicates significant correlations. (* P < 0.05, ** P < 0.01)

(Abbreviations: EC, electrical conductivity; Cl, chloride; Na, sodium; Cu, copper; Fe, iron; Mn, manganese; Zn, zinc; NN, nitrate nitrogen; AN, ammonium nitrogen; P, phosphorus; OM, organic matter; TC, total carbon; TN, total nitrogen)

Figure captions

Figure 1 Classification of the ARGs (a) and resistance mechanisms of the ARGs (b) in all the beach soil samples based on the numbers of detected ARGs; The relative abundance of ARGs and MGEs among all the samples (c) and in each sampling site (d). (Abbreviations: MLSB, macrolide-Lincosamide-Streptogramin B resistance; FCA, fluoroquinolone, quinolone, florfenicol, chloramphenicol, and amphenicol resistance genes).

Figure 2 The heatmap showing the relative abundance of individual ARG and MGE subtypes detected across soil samples. The classes of ARG subtypes and core resistome are labelled on the right. (Abbreviations: MLSB, macrolide-Lincosamide-Streptogramin B resistance; FCA, fluoroquinolone, quinolone, florfenicol, chloramphenicol, and amphenicol resistance genes).

Figure 3 The bacterial community compositions at the phylum level among all the samples (a) and individual sampling sites (b). The relative abundance of the top 20 bacterial classes (c), the boxes are colored according to their respective phyla.

Figure 4 (a) The percentage of the number and relative abundance of core resistome compared to the total ARGs; (b) The taxonomic composition of the core resistome (only dominant ARG subtypes in each class are labelled); (Abbreviations: MLSB, macrolide-Lincosamide-Streptogramin B resistance; FCA, fluoroquinolone, quinolone, florfenicol, chloramphenicol, and amphenicol resistance genes).

Figure 5 The networks showing the co-occurrence patterns among ARGs and MGEs based on the correlation analysis. The nodes with different colors represent (a) different categories of ARGs and (b) different modules. Node size is proportional to the number of connections; edge width is proportional to Spearman's ρ value. (Abbreviations: MLSB, macrolide-Lincosamide-Streptogramin B resistance; FCA, fluoroquinolone, quinolone, florfenicol, chloramphenicol, and amphenicol resistance genes).

Figure 6 Comparison of the relative abundance of ARGs (a, b, c) and MGEs (d, e, f) along the salinity gradients of sodium (a and b), chloride (c and d) and electrical conductivity (e and f). Significant difference is represented by different letters above the boxes ($P < 0.05$). (Abbreviations: EC, electrical conductivity)

Figure 7 Structural equation modelling of the effects of MGEs, soil salinity, soil fertility, heavy metal, microbial community and sample type on the profiles of ARGs (a). The goodness-of-fit statistics are: $\chi^2 = 12.8$, P = 0.12, RMSEA = 0.049, CFI = 0.48. Solid and dash lines represent positive and negative effects, respectively. The line width is proportional to the strength of the standardized path coefficients (as indicated by the numbers adjacent to lines). The R^2 value indicates the proportion of variance explained by the variable. *$P < 0.05$, ** $0.05 < P < 0.01$, ***$P < 0.001$. (b) Standardized total effects (sum of direct and indirect effects) of the major factors on the ARG profiles based on the SEM results. (Abbreviations: EC, electrical conductivity; P, phosphorus; TC, total carbon; Cl, chloride; Na, sodium; TN, total nitrogen; Mn, manganese; MGEs, mobile genetic elements).

Figure 1

Click here to download high resolution image

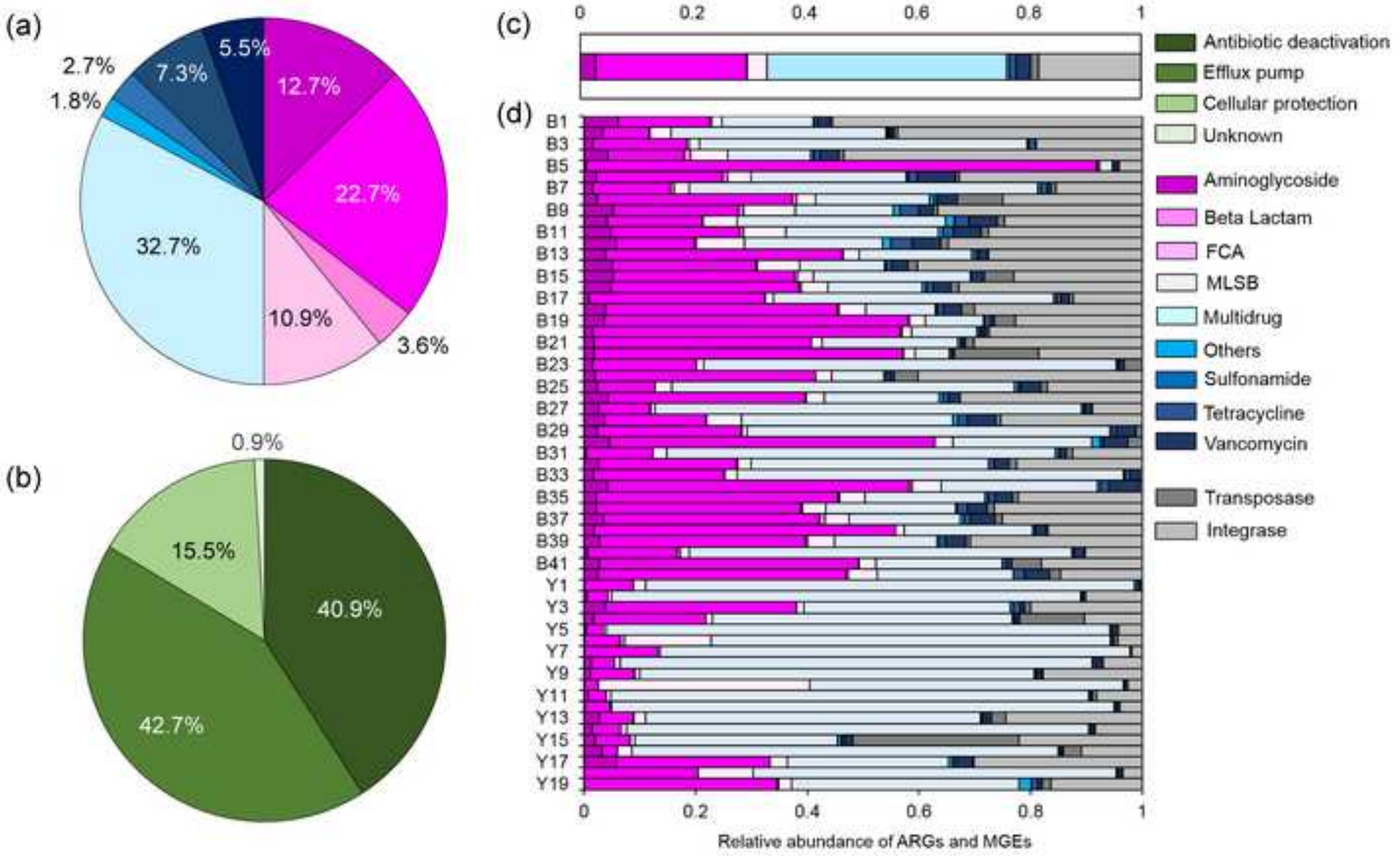

Figure 2

Click here to download high resolution image

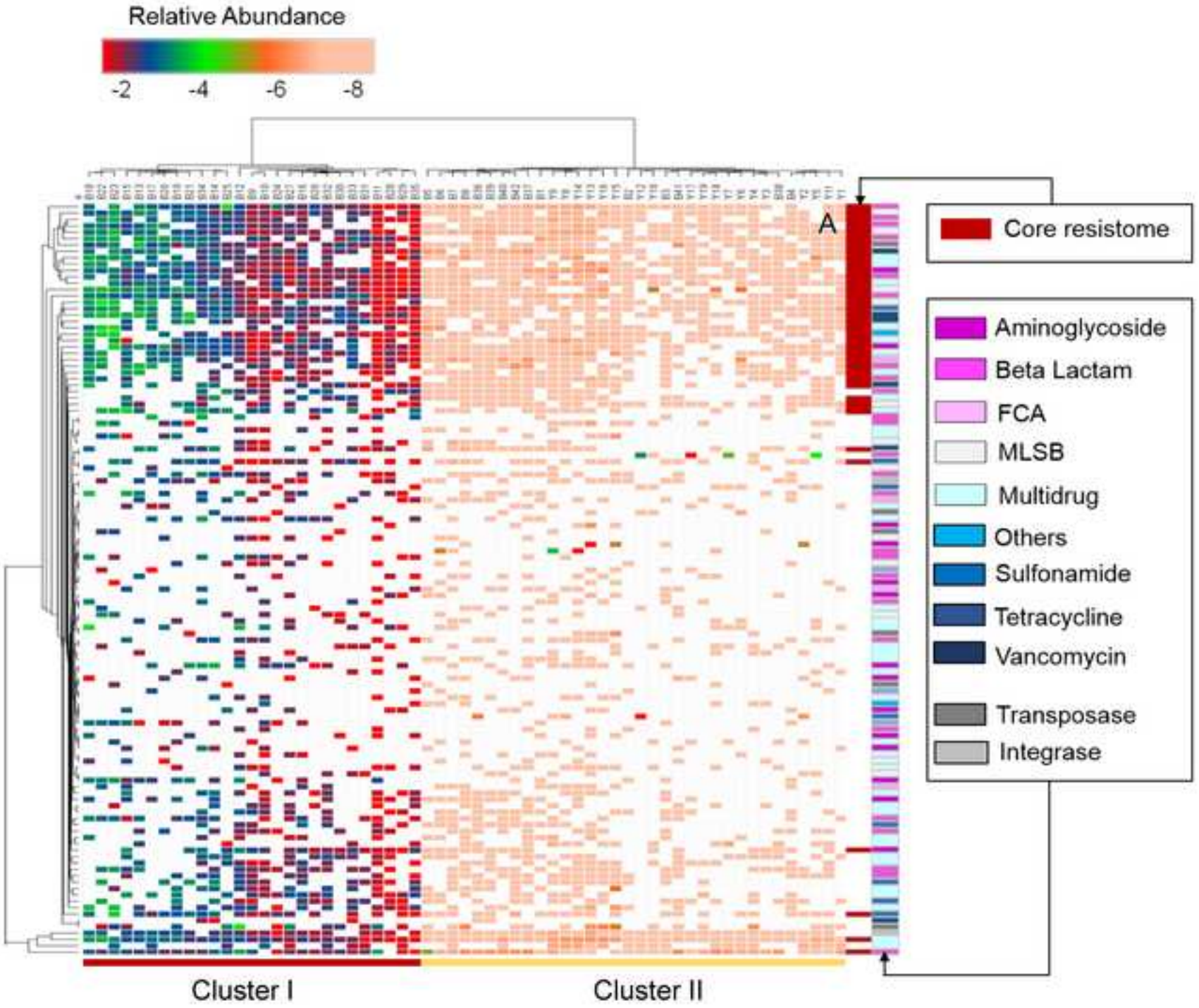

Figure 3

Click here to download high resolution image

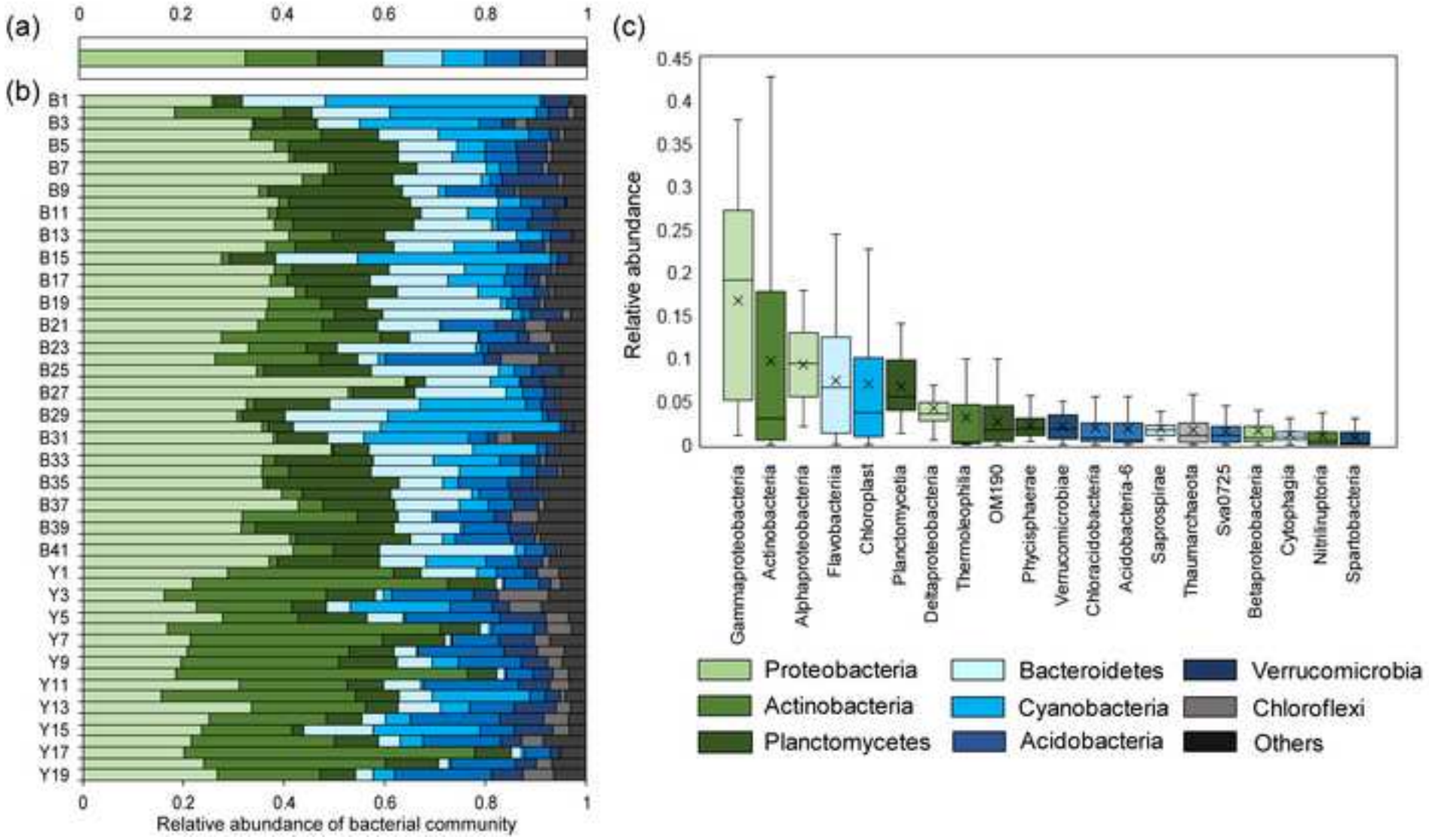

Figure 4

Click here to download high resolution image

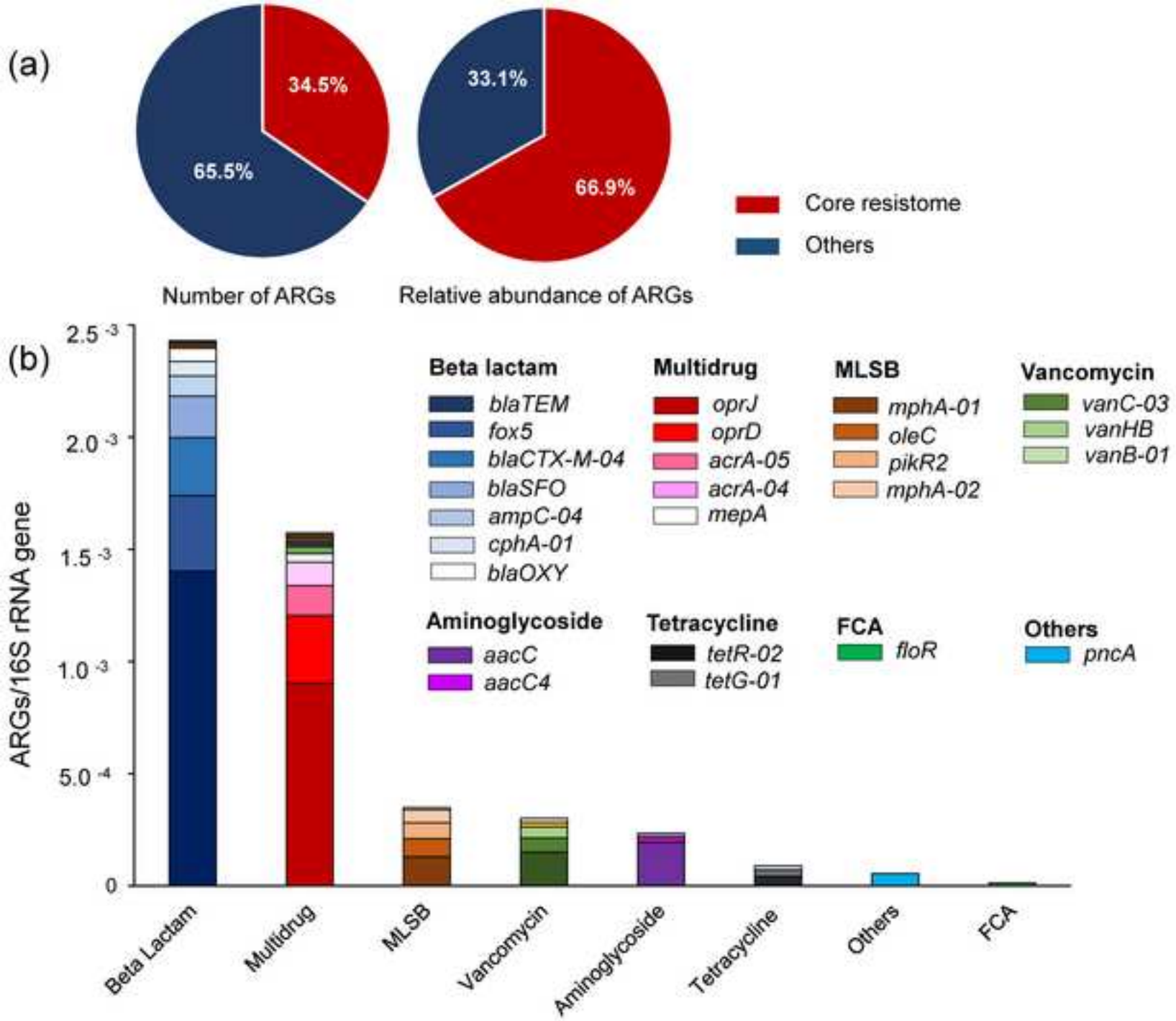

Figure 5

Click here to download high resolution image

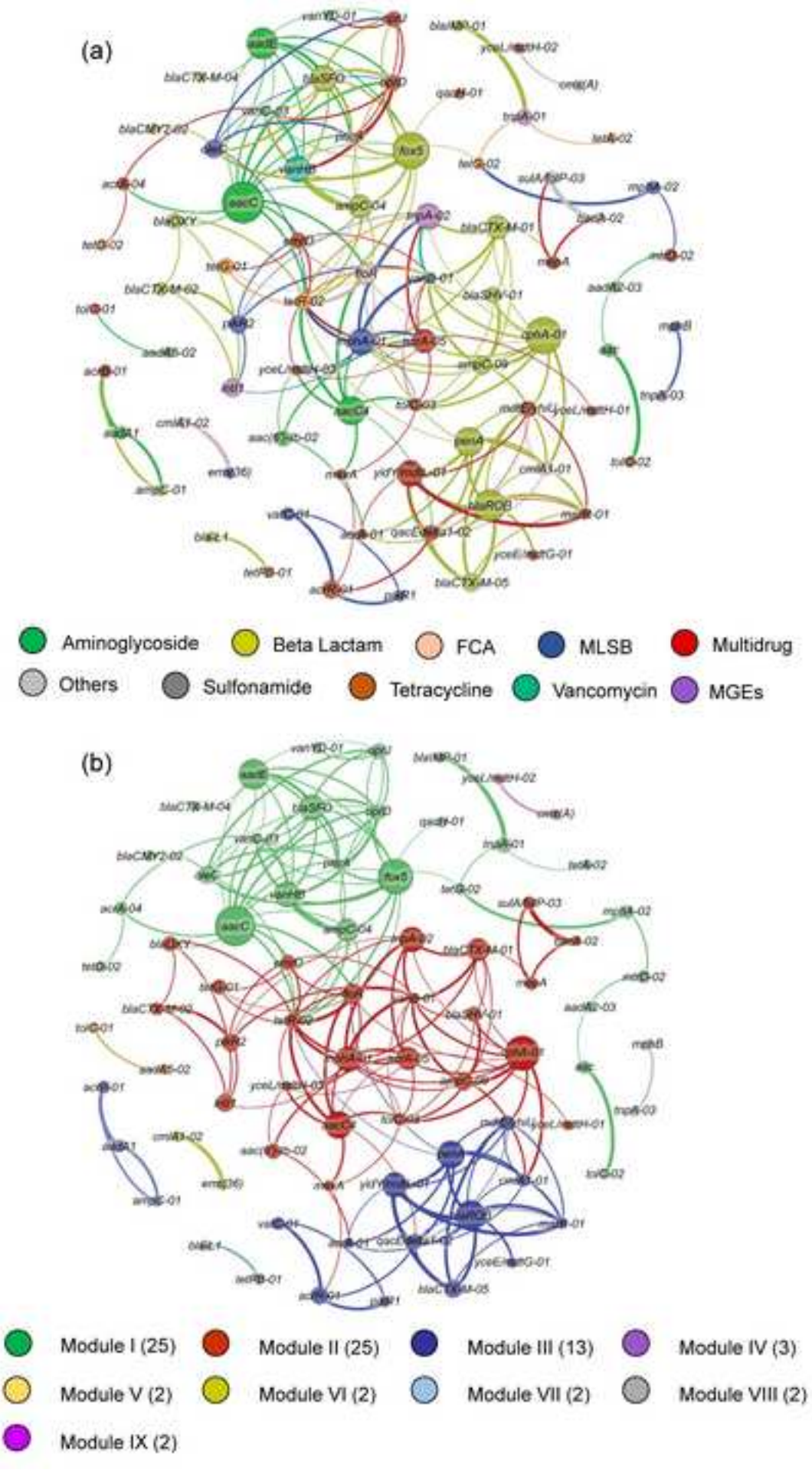

Figure 6

Click here to download high resolution image

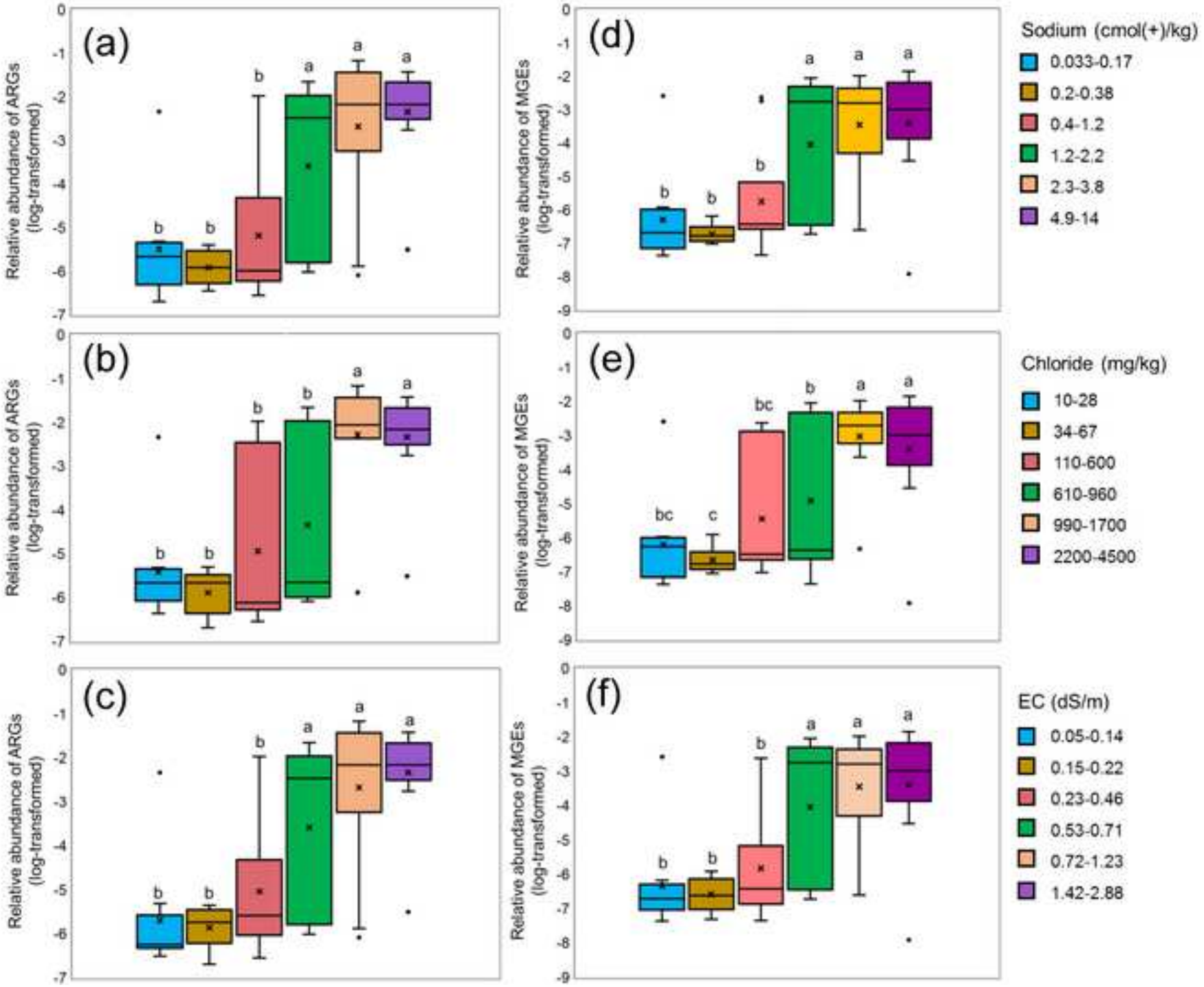

Figure 7

Click here to download high resolution image

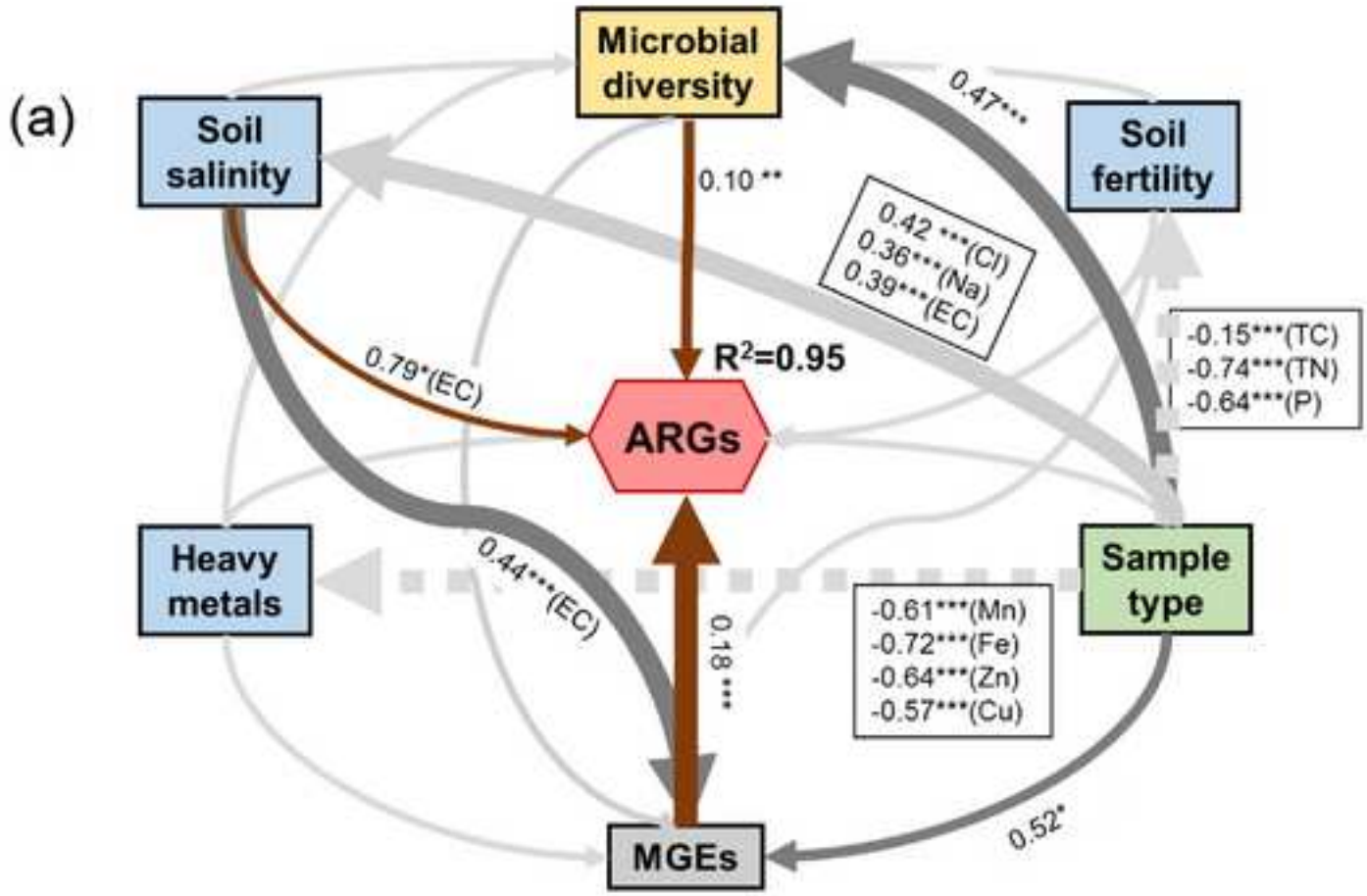

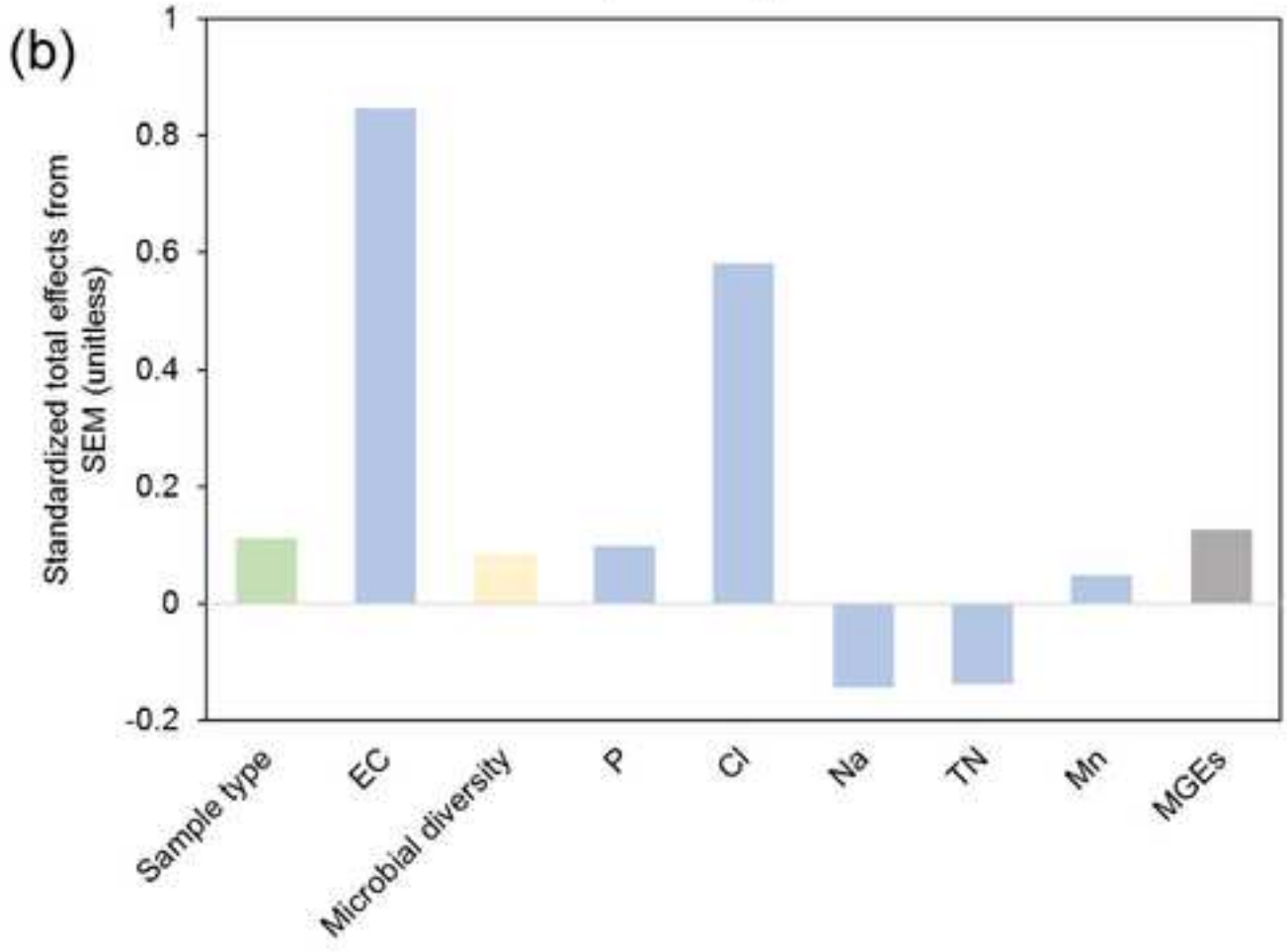

Supplementary material for on-line publication only

Click here to download Supplementary material for on-line publication only: Supplementary information.doc